



Original article

Hybrid Silver Nanoparticles–Purple Sweet Potato (*Ipomoea batatas* L.) Peels as a Prospective Adsorbent for Bromophenol Blue Removal

Mirza Ardella Saputra^{1,2,*}, Bastoni Semendawai¹, and Mochamad Lutfi Firmansyah^{1,2}

¹Nanotechnology Engineering, Faculty of Advanced Technology and Multidiscipline, Universitas Airlangga, Surabaya 60115, Indonesia

²Airlangga Functional Nanomaterials Research Group, Faculty of Advanced Technology and Multidiscipline, Universitas Airlangga, Surabaya 60115, Surabaya

Received 12 April 2025; Accepted 16 May 2025

*Corresponding author: mirza.ardella@ftmm.unair.ac.id

Abstract—Water pollution caused by dye effluents has become a global problem, for example in the textile, paper, and food industries. One common type of dye waste is bromophenol blue, which is considered to pose a low level of danger, but frequent exposure to its waste can cause skin irritation. This research was conducted using silver nanoparticles synthesized with purple sweet potato (*Ipomoea batatas* L.) peels (IBpe), which are rich in anthocyanin content so that it can be used as an active reducing agent and produce an adsorbent used for dye waste removal. Combination of biogenic-chemical method was chosen due to its simplicity, cost-effectiveness, and lower toxicity. Characterization of the obtained nanomaterials included UV-Vis spectroscopy, FTIR, SEM-EDX, and XRD. The results showed that the average crystal size of IBpe-AgNPs of 1:3, 1:5 and 1:9 were 7.09 nm, 8.68 nm, and 13.99 nm, respectively, with an FCC crystal shape. The average particle sizes of AgNPs in three IBpe-AgNPs variations were 82.76 nm, 85.72 nm, and 99.78 nm, respectively, with each showed a spherical shape. The research found that IBpe-AgNP 1:9 demonstrated the highest adsorption efficiency of 77.24% compared to the other samples. In terms of desorption efficiency, the IBpe-AgNP 1:3 sample showed the highest value at 75.54% compared to the other three samples. Furthermore, the reuse test revealed that the IBpe-AgNP 1:9 sample had the highest reuse value at 27.02% compared to the other samples, showing the same trend as the first adsorption.

Keywords— hybrid silver nanoparticles, *Ipomoea batatas*, biogenic method, adsorption, bromophenol blue, pollutant removal.

I. INTRODUCTION

Water pollution is a global issue, affecting both households and industries, with dye contamination being a major concern, especially in industries like textiles, cosmetics, and food. Dyes are among the top three global pollutants, with over 700,000 tons used annually in the textile industry alone [1,2]. These contaminants hinder water reoxygenation, block sunlight

penetration, and pose toxic risks to aquatic life [3]. Additionally, they can be carcinogenic and mutagenic, leading to severe health issues in humans [4]. One common pollutant is bromophenol blue (BB), widely used in various industries [5,6]. While several methods exist to remove organic dyes, many are costly and ineffective [2,7]. Adsorption is considered the most efficient and economical solution, but it requires suitable adsorbents for effective water treatment [8,9].

Adsorbents are solid materials that attract contaminants from water to their surface during adsorption. Effective adsorbents must be water-insoluble, have high affinity for pollutants, and be easily regenerated [10]. Organic, inorganic, and biomass-based adsorbents (bio-sorbents) are commonly used, with bio-sorbents favored for their low cost, biodegradability, and efficiency [11,12]. Their performance can be enhanced with nanomaterials, particularly silver nanoparticles (AgNPs), which offer excellent physicochemical properties, high surface area, and unique characteristics [13]. AgNP hybrids, combining silver nanoparticles with organic biomass materials, are eco-friendly, highly efficient in removing pollutants, and easily recyclable, making them promising adsorbents for water treatment.

The organic material used for the AgNP hybrid synthesis in this study is purple sweet potato (*Ipomoea batatas* L.), known for its high nutritional value and natural bioactive compounds [14,15]. Its peel (*Ipomoea batatas* peel – IBpe) is an industrial byproduct that remains largely underutilized, despite its high and stable anthocyanin content compared to other tubers [16,17]. The abundance and stability of anthocyanins make it an effective reducing agent for AgNP synthesis. Previously, IBpe has been utilized to synthesize AgNPs with various assays [14,16], but has not been used as IBpe-AgNP hybrid. Herein we report the synthesis of IBpe-AgNP that will serve as a bio-sorbent for removing organic dyes, particularly bromophenol

blue (BB), with three variations of IBpe biomass concentrations tested. Therefore, not only we would utilize the commonly wasted sweet potato peels that are common in Asia, we can also further utilize them in water purification via adsorption method.

The preparation of IBpe-AgNP involves mixing an AgNO₃ solution with IBpe powder in ratios of 1:3, 1:5, and 1:9. Trisodium citrate is then added to aid anthocyanins in reducing AgNO₃ into AgNP. The produced IBpe-AgNP is characterized using UV-Vis spectroscopy, XRD, FTIR, and SEM-EDX. Decontamination tests are conducted by adding contaminant solutions to determine the bio-sorbent's adsorption efficiency. Desorption tests then performed using NaOH to measure the desorption percentage. The bio-sorbent samples are then reused in another decontamination test to assess their reusability.

II. EXPERIMENTAL SECTION

A. Materials

Materials needed for this research include purple sweet potatoes (*Ipomoea batatas* L.) obtained from Pasar Kali, Surabaya, Indonesia; silver nitrate (AgNO₃, Sigma Aldrich, ACS Reagent); trisodium citrate dihydrate (C₆H₅Na₃O₇•2H₂O, Sigma Aldrich, ACS Reagent); bromophenol blue (C₁₉H₁₀Br₄O₅S, Sigma Aldrich, ACS Reagent); hydrochloric acid (HCl, 37%, Smart-Lab); and sodium hydroxide (NaOH, Supelco, >99%).

B. Instrumentations

Instruments used for characterization include UV-Vis spectrophotometer (GENESYS 40/50, Thermo-Scientific, USA), Fourier Transform Infrared Spectroscopy (FTIR, Nicolet iS 10, Thermo-Scientific, USA), X-Ray Diffraction (XRD, Miniflex 600, Rigaku, Japan), and Scanning Electron Microscope-Energy Dispersive X-Ray (SEM-EDX, Phenom proX, Thermo-Scientific, USA).

C. Preparation of purple sweet potato peels (IBpe)

Sweet potatoes (*Ipomoea batatas* L.) were peeled using knife and the peels were washed under running water to remove the excess dirt. The peels were cut into smaller pieces and sun dried for 24 h. Then, these peels were dried in a dehydrator (LocknLock EJO316) at 80 °C for 6 h to complete the drying process. Once dried, the peels were crushed using mortar and pestle and sieved to get IBpe powder in 100 µm size.

D. Synthesis and characterization of hybrid silver nanoparticles – purple sweet potato peels (IBpe-AgNP)

The hybrid silver nanoparticles-purple sweet potato peels were prepared following previous reported method with some modification [18]. Three mass ratio variations of AgNO₃:IBpe powder were prepared using 50 mL of 23 mM AgNO₃ solution in distilled water. The IBpe powder added for 1:3, 1:5, and 1:9 variations were 0.638 g, 1.063 g, and 1.913 g, respectively. The mixture of the AgNO₃ solution and IBpe was each stirred for 2 h, and 3 mL of 1% b/v trisodium citrate dihydrate solution was then added to the mixture. Additional 16 h was added to stir the mixture at room temperature to complete the formation of

AgNP on IBpe. After stirring, the mixture was centrifuged at 4000 rpm for 1 h and the precipitate was washed with 5% ethanol until neutral. The obtained solid was dried using dehydrator at 70 °C for 24 h, grind into fine powder using mortar and pestle, and sieved to get IBpe-AgNP 1:3, 1:5, and 1:9 in 100 µm size.

E. Adsorption of bromophenol blue

First, stock solution of 50 ppm bromophenol blue (BB) solution was prepared and adjusted to pH 4 using 1M HCl. As much as 50 mg of the IBpe-AgNP was added to 10 mL of 50 ppm BB solution and sonicated using water bath sonicator at 27 °C for 150 minutes, with sampling every 30 minutes. Then, the mixture was centrifuged at 4000 rpm for 30 minutes. The filtrate was analyzed using spectrophotometer UV-Vis to observe the residual BB at 590 nm. The concentration of the residual BB was calculated following calibration curve using five different concentration BB solution of 100 ppm, 50 ppm, 25 ppm, 12.5 ppm, and 6.25 ppm. Percent adsorption of BB and capacity uptake of the bio-sorbent were calculated following (1) and (2).

$$\% \text{ adsorption} = \frac{C_i - C_e}{C_i} \times 100 \quad (1)$$

$$q_e = \frac{V(C_i - C_e)}{m} \quad (2)$$

with C_i (ppm) is initial concentration of BB; C_e (ppm) is BB concentration after adsorption; q_e (mg/g) is capacity uptake; V (L) is volume of the working solution; and m (g) is the amount of the added adsorbent. The adsorption of BB was carried out to the three variations of IBpe-AgNP and bare IBpe as comparison, each in triplication.

F. Regeneration and reusability

Following the adsorption of BB, the solid bio-sorbent containing BB was separated from the liquid and dried in a dehydrator at 80 °C for 40 minutes. Then, the bio-sorbent was added to 10 mL of 0.5 M NaOH desorption solution and sonicated using water bath sonicator at 27 °C for 30 minutes. The amount of desorbed BB in the alkaline solution was analyzed using spectrophotometer UV-Vis and calculated using (3).

$$\% \text{ desorption} = \frac{C_D V_D}{q_e m} \times 100 \quad (3)$$

with q_e (mg/g) is the initial capacity uptake; m (g) is the amount of the added adsorbent; C_D (ppm) is concentration of BB after desorption; and V_D (L) is the volume of the desorption solution. The regenerated adsorbent was used for reusability test after drying it in a dehydrator at 80 °C for 40 minutes. The second BB adsorption was performed following the first method, and carried out to the three variations of IBpe-AgNP and bare IBpe as control.

III. RESULTS AND DISCUSSION

The hybrid bio-sorbent IBpe-AgNP was prepared utilizing purple sweet potato peels that usually became domestic waste [19]. Polyphenols, especially anthocyanin, should still be presence in the peels (IBpe) since purple sweet potatoes are

known to have various natural product compounds in all parts of the plants [17]. However, due to the drying process and the absence of extraction process, the synthesis of silver nanoparticles could not be done without the addition of trisodium citrate dihydrate as chemical reductor to reduce Ag^+ to Ag^0 . This was proven by a reaction carried out without the addition of trisodium citrate dihydrate that showed no changes of the silver nitrate precursor. Therefore, the addition of trisodium citrate dihydrate plays a big role to the in-situ formation of AgNPs impregnated on the IBpe [20]. The visual representations of the reaction are shown at Fig. 1, in which each reaction mixture shows a brownish color with the IBpe-AgNP 1:3 being the darkest, despite being the smallest amount of IBpe added. The brown powder of the IBpe concealed the usual AgNPs color of yellow due to the surface plasmon resonance properties [21]. The obtained dried powder of IBpe-AgNP also showed similar trend of color with variations 1:3 being the darkest brown and 1:9 being the lightest brown.

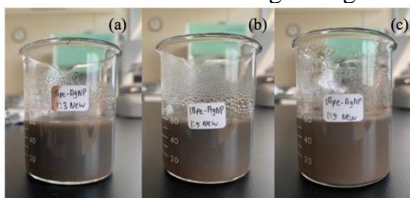


Figure 1. Visual representations of IBpe-AgNP a) 1:3 b) 1:5 c) 1:9

Analysis with spectrophotometer UV-Vis of the IBpe-AgNP solutions was performed to identify the presence of silver nanoparticles, as seen in Fig. 2. Bare IBpe (black line) showed double peak at 280-350 nm wavelength, indicated the common peak for polyphenols in plants, such as flavonoids and anthocyanins [17]. Meanwhile, the IBpe-AgNP 1:3 and 1:5 samples (red and blue line, respectively) each showed a broad peak around 450 nm, while IBpe-AgNP 1:9 (green line) did not really show any distinct peak at the same wavelength. The broadness of the peak presumably due to the overlapping peak of the expected silver nanoparticles and the excess compounds from IBpe that possible to be extracted during the stirring process of 24 h. However, based on this spectrum, we can somewhat see where silver nanoparticles normally show up at wavelength range of 390-450 nm [21]. Despite the low absorbance values, the UV-Vis spectrum showed a trend of the more the IBpe added, the higher the absorbance of the expected silver nanoparticles being synthesized.

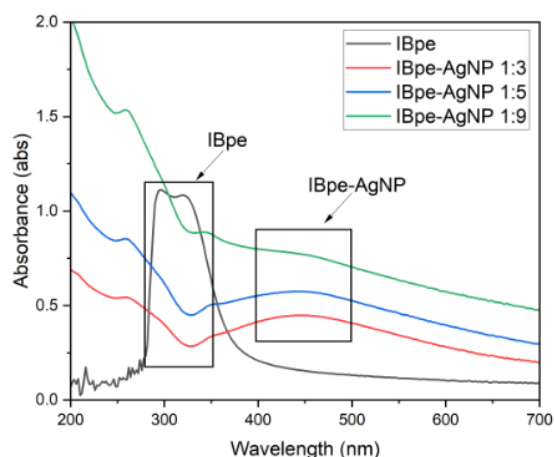


Figure 2. UV-Vis spectrum of IBpe (black), IBpe-AgNP 1:3 (red), IBpe-AgNP 1:5 (blue), and IBpe-AgNP 1:9 (green)

To confirm that silver nanoparticles are indeed successfully synthesized, analysis using XRD was also conducted. XRD analysis was carried out at 2θ range of $10-80^\circ$ and the results can be seen at Fig. 3. As expected, IBpe (black line) revealed a broad peak implying amorphous material because IBpe only consists of organic compounds [18]. IBpe-AgNP 1:3 (red line) showed diffraction pattern at 38° , 44.40° , 64.40° , and 77.26° , while IBpe-AgNP 1:5 (blue line) and IBpe-AgNP 1:9 (green line) showed exact pattern at 38° , 44.20° , 64.40° , and 77.30° . Based on these diffraction patterns that similar to Joint Committee on Powder Diffraction Standards (JCPDS) file no. 84-0713, we can confirm that silver nanoparticles were successfully synthesized using this method, with the crystalline phase of cubic FCC with crystal lattice structure of (111), (200), (220), and (311) [14]. The different amount of IBpe being added did not interfere the formation of AgNPs that displayed on the XRD diffraction patterns. All three variations showed up at the same 2θ with similar intensity. Based on the Williamson-Hall plot calculation, the average crystal size (and microstrain) of IBpe-AgNP 1:3, 1:5, and 1:9 were 7.09 nm (2.62 nm), 8.68 nm (1.8 nm), and 13.99 nm (1.08), respectively. These results showed that the crystalline sizes are in reverse of the microstrain values, meaning that when the crystalline size is bigger, the microstrain value is smaller, as the boundaries between crystallite can introduce stress and strain. Conversely, larger crystallite but having lower microstrain value as in IBpe-AgNP 1:9 perhaps suggesting a more ordered and less distorted lattice structure. All these could affect the adsorption properties.

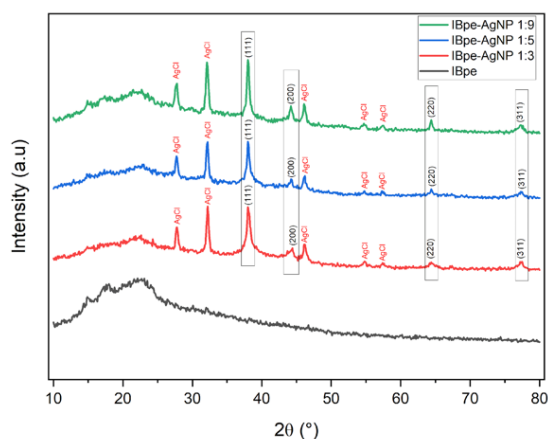


Figure 3. XRD patterns of IBpe (black), IBpe-AgNP 1:3 (red), IBpe-AgNP 1:5 (blue), and IBpe-AgNP 1:9 (green)

As also seen in Fig. 3, AgNPs were not the only product observed in this synthesis. There are obvious diffraction patterns at 2θ of 27.80° , 32.19° , 46.13° , 54.81° , and 57.40° for IBpe-AgNP 1:3; 2θ of 27.69° , 32.21° , 46.19° , 54.78° , and 57.29° for IBpe-AgNP 1:5; and 2θ of 27.78° , 32.09° , 46.11° , 54.69° , and 57.50° for IBpe-AgNP 1:9. After examination with by comparing with literatures, these peaks contributed to AgCl that was formed due to the reaction between Ag^+ from AgNO_3 with Cl^- from the IBpe biomass. Similar observations has been reported previously from the use biomasses of *Oedera genitifolia*, *Benincasa hispida*, and traditional Chinese medicine plants [22-24]. These results suggesting a competing reaction of Ag^+ from AgNO_3 to be reduced to Ag^0 or to form a new ionic reaction to form AgCl, which almost 1:1 by looking at the intensity of the diffraction patterns.

The next analysis being used to characterize hybrid bio-sorbent IBpe-AgNP was FT-IR, as seen in Fig. 4. Pristine IBpe and three IBpe-AgNP variations were analyzed using KBr pellet. All four spectrums showed similar pattern of bands and wavenumbers at $500\text{--}4000\text{ cm}^{-1}$, suggesting that they have same functional groups with similar intensities, most likely from IBpe. Meanwhile, the possible bands of AgNP and AgCl were not really observable at wavenumber below 500 cm^{-1} . The four functional groups noted from the spectrum were broad band of -OH vibration at 3420 cm^{-1} , C-H stretching at 2926 cm^{-1} , C=C stretching vibration at 1640 cm^{-1} , and C-O stretching vibration at 1020 cm^{-1} . All these bands signifying the presence of phenolic compound in IBpe, especially anthocyanin [14].

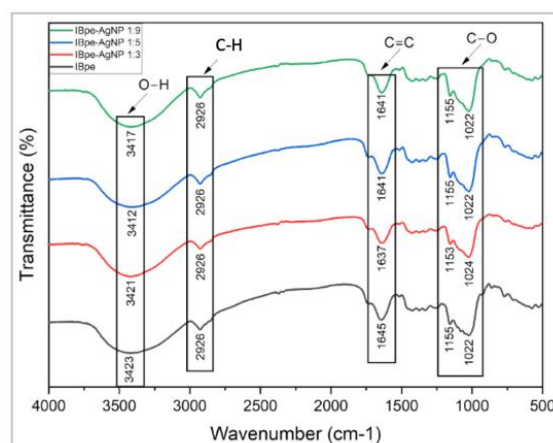


Figure 4. FT-IR spectrum of IBpe (black), IBpe-AgNP 1:3 (red), IBpe-AgNP 1:5 (blue), and IBpe-AgNP 1:9 (green)

Lastly, SEM-EDX was used to understand the surface morphology of the bio-sorbent, the average diameter of AgNPs, and the element composition of each sample. Fig. 5(a) displayed the image of IBpe to have a smooth surface without white dots observed, while Fig. 5(b-d) showed IBpe-AgNP of the three variations having a rougher surface with white dots of AgNP are observed. These revealed that AgNP are formed on the surface of the IBpe with spherical shape, similar to the literature [21]. While the AgNO_3 precursor used during synthesis was remained constant, apparently the addition of IBpe affected the amount of the obtained AgNPs. The trend of the obtained AgNPs were in agreement of the UV-Vis spectroscopy method, in which the IBpe-AgNP 1:9 presumably having the most AgNPs presence based on the absorbance value as well as based on the SEM image. Through some calculation using ImageJ software, the particle sizes of the AgNPs on IBpe-AgNP 1:3, 1:5, and 1:9 were 82.76 nm , 85.72 nm , and 99.78 nm , respectively. These were also aligned with the XRD results. These calculations' histogram also suggested that IBpe-AgNP 1:9 had the most homogenic result of AgNPs.

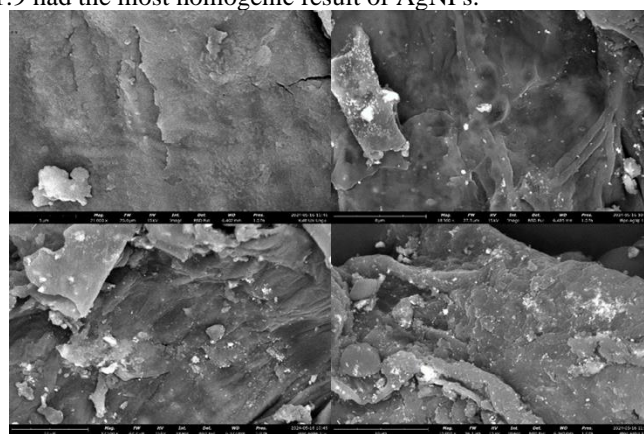


Figure 5. SEM images of a) IBpe b) IBpe-AgNP 1:3 c) IBpe-AgNP 1:5 and d) IBpe-AgNP 1:9

Based on the EDX analysis on Table 1 pure IBpe only showed elements of C, O, K, Cl, and S. IBpe-AgNP variation 1:3

showed same elements as of pure IBpe with addition of Ag element observed in 6.9% while IBpe-AgNP 1:5 showed 8.1% of Ag. Lastly, IBpe-AgNP 1:9 unfortunately showed a lower Ag in 6.6%. IBpe-AgNP 1:9 supposedly having more surface area of IBpe because higher amount of IBpe was added to the variation, which then caused AgNP to spread even more and possibly not observed during EDX analysis on random areas. Despite that, these element composition analyses supported the conclusion that AgNPs was successfully impregnated onto IBpe surface, while the detected chloride also supported the previous characterization results using XRD.

Table 1. Element percentages based on SEM-EDX analysis

Element	IBpe	IBpe-AgNP		
		1:3	1:5	1:9
C	59.7%	58%	51.4%	59%
O	30.6%	33.2%	38.6%	30.9%
Ag	-	6.9%	8.1%	6.6%
Cl	2.2%	1.2%	0.5%	1.2%
K	6.5%	0.1%	0.8%	1.1%
S	0.7%	0.3%	0.3%	0.9%

To test the ability of the prepared bio-sorbent IBpe-AgNP, we contacted 50 mg of each hybrid bio-sorbent with 10 mL of 50 ppm BB solution for 150 minutes using water bath sonicator, with sampling every 30 min. Visually, the BB solution in pH 4 changed from the initial magenta color to turbid purple color after the decontamination process using each variation of IBpe-AgNP. In contrast, IBpe control was remained magenta and visibly clearer. As seen in Fig. 6a, the BB adsorption happened quick at the first 5 minutes for all four samples, with each showed irregular % adsorption on the 30 minutes and 60 minutes marks, where they showed decrease instead of increasing % adsorption. However, on the 90 minutes forward the adsorption showed increments, especially for IBpe-AgNP 1:9. The changes of the UV-Vis spectrum of before and after 150 minutes sonication is shown in Fig. 6(b).

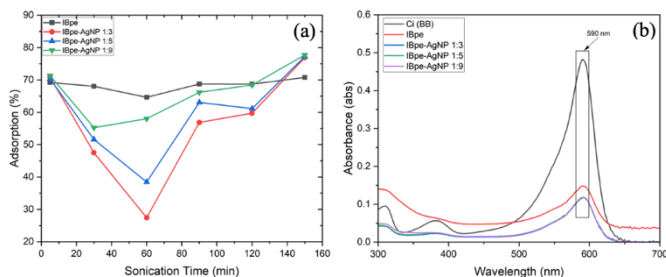


Figure 6. a) Percent adsorption of each sample every 30 min. b) UV-Vis spectrum of BB before and after 2 h

Results of the % adsorption and capacity uptake of each sample are detailed in Table 2. Unmodified IBpe showed 70.71% adsorption of BB and 8.84 mg/g capacity uptake, while addition of AgNPs increased the % adsorption and capacity uptake to 76.89% (9.61 mg/g), 77.24% (9.75 mg/g), and 77.70% (9.71 mg/g), respectively. These results showed that IBpe on its own have properties to remove BB from water with constant adsorption from minute 5 to minute 150, but stayed

constant at 70%. Meanwhile, the addition of AgNPs improved the properties to adsorb BB to 78% with IBpe-AgNP 1:9 being the best of four tested samples. This is aligned with the results of characterization of the hybrid nanomaterials, which also supported by the highest addition of IBpe provided more active site to adsorb BB. Perhaps by adding more time of contact between the bio-sorbent with BB solution, percent adsorption and capacity uptake of IBpe-AgNP 1:9 could be increased to near 100%.

Table 2. Percent adsorption and capacity uptake results

Variation	% Adsorption	Capacity Uptake (mg/g)
IBpe	70.71	8.84
IBpe-AgNP 1:3	76.89	9.61
IBpe-AgNP 1:5	77.24	9.65
IBpe-AgNP 1:9	77.70	9.71

The desorption process was then performed to the BB-contained hybrid bio-sorbent using 0.5 M NaOH as the desorption solution. After the addition of IBpe and three variations of IBpe-AgNP, the mixture was clear with purplish or yellowish color that changed to clear yellow mixture for the IBpe, and turbid yellowish mixture for the IBpe-AgNP variations. These color visually, combined with the UV-Vis spectrum as seen in Fig. 7(a), indicating that some of the AgNPs were detached from the composites. The strong presence of peak at 415 nm for IBpe-AgNP suggested the peak of AgNPs, while the BB peak that should be on 590 nm did not visible. Eventually, the obtained solid was tested again in the adsorption of BB as shown in Fig. 7(b), the peak of BB was present at 590 nm along with peak at 415 nm.

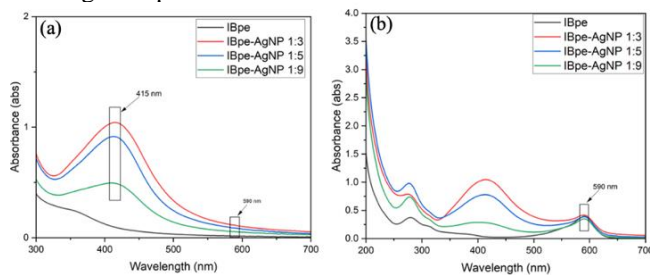


Figure 7. a) Desorption UV-Vis spectrum and b) Reusability in adsorption of IBpe (black), IBpe-AgNP 1:3 (red), IBpe-AgNP 1:5 (blue), and IBpe-AgNP 1:9 (green)

Removal of BB using IBpe-AgNP is proposed to follow the physisorption mechanism where it could be reversible, temperature dependent, and weak bonding between adsorbent and adsorbate, such as electrostatic interaction [18]. This gives a more accessible regeneration and reusability of the adsorbent. However, this needs to be confirmed by calculating the kinetics or computation to understand the adsorption mechanism. In this research, the desorption efficiency showcased the opposite results than the adsorption efficiency as in Table 3, where IBpe-AgNP 1:3 had the biggest percent desorption at 27.54%, followed by IBpe-AgNP 1:5 at 20.04%, and IBpe-AgNP 1:9 at 11.60%. This desorption process could happen when the acidic adsorbed sample reacted with alkaline solvent, ion exchange

could occur and the BB was released from the hybrid IBpe-AgNP [10,18]. Finally, the regenerate adsorbate was reused in the BB adsorption and the results showed similar trend as the first adsorption, in which IBpe-AgNP showcased the highest percent adsorption at 27.02% compared to the others, including IBpe. Nevertheless, these results confirm that hybrid bio-sorbent combination of IBpe and AgNP could be used as prospective adsorbent for the removal of organic dye from water. Further adsorption tests need to be performed at different conditions, including testing towards various other organic dyes.

Table 3. Desorption and reusability results

Variation	% Desorption	Reusability (%)
IBpe	0.83	17.66
IBpe-AgNP 1:3	27.54	13.45
IBpe-AgNP 1:5	20.04	19.71
IBpe-AgNP 1:9	11.60	27.02

CONCLUSION

This study utilizes combination of biogenic-chemical method to synthesize composite of silver nanoparticle decorated on purple sweet potato (IBpe) peels, that not only eco-friendly but also simple and low cost. Utilization of purple sweet potato peels also improve the usage of food scraps as bio-sorbent that was successfully enhanced with the addition of AgNPs. The produced IBpe-AgNPs were confirmed using various characterization techniques, especially XRD and SEM-EDX. These hybrid IBpe-AgNPs showed increasing percent adsorption of BB as organic dye pollutant sample. In summary, this study provided a basis for the future usage of biomass-supported AgNPs such as IBpe-AgNPs, which could be promising in the development of new material as adsorbent for water pollution treatment.

ACKNOWLEDGMENT

Mirza Ardella Saputra acknowledges the financial support by Airlangga Research Fund (ARF) Universitas Airlangga 2023 through an Early Career Research Grant Scheme (No. 417/UN3.1.17/PT/2023).

REFERENCES

- [1] I. A. Aguayo-Villarreal, D. Cortes-Arriagada, C. K. Rojas-Mayorga, K. Pineda-Urbina, R. Muñiz-Valencia, and J. González, "Importance of the interaction adsorbent-adsorbate in the dyes adsorption process and DFT modeling," *J. Mol. Struct.*, vol. 1203, p. 127398, Mar. 2020, doi: 10.1016/j.molstruc.2019.127398.
- [2] V. Katheresan, J. Kansedo, and S. Y. Lau, "Efficiency of various recent wastewater dye removal methods: A review," *J. Environ. Chem. Eng.*, vol. 6, no. 4, pp. 4676–4697, Aug. 2018, doi: 10.1016/j.jece.2018.06.060.
- [3] S. Senthilkumar, P. Kalaamani, K. Porkodi, P. R. Varadarajan, and C. V. Subburaam, "Adsorption of dissolved Reactive red dye from aqueous phase onto activated carbon prepared from agricultural waste," *Bioresour. Technol.*, vol. 97, no. 14, pp. 1618–1625, Sep. 2006, doi: 10.1016/j.biortech.2005.08.001.
- [4] K. G. Akpomie and J. Conradie, "Efficient synthesis of magnetic nanoparticle-*Musa acuminata* peel composite for the adsorption of anionic dye," *Arab. J. Chem.*, vol. 13, no. 9, pp. 7115–7131, Sep. 2020, doi: 10.1016/j.arabjc.2020.07.017.

- [5] J. Liu, S. Yao, L. Wang, W. Zhu, J. Xu, and H. Song, "Adsorption of bromophenol blue from aqueous samples by novel supported ionic liquids," *J. Chem. Technol. Biotechnol.*, vol. 89, no. 2, pp. 230–238, Feb. 2014, doi: 10.1002/jctb.4106.
- [6] Q. Liu, "Pollution and Treatment of Dye Waste-Water," *IOP Conf. Ser. Earth Environ. Sci.*, vol. 514, no. 5, p. 052001, May 2020, doi: 10.1088/1755-1315/514/5/052001.
- [7] N. S. Shah *et al.*, "Nano-zerovalent copper as a Fenton-like catalyst for the degradation of ciprofloxacin in aqueous solution," *J. Water Process Eng.*, vol. 37, p. 101325, Oct. 2020, doi: 10.1016/j.jwpe.2020.101325.
- [8] M. N. Zafar, Q. Dar, F. Nawaz, M. N. Zafar, M. Iqbal, and M. F. Nazar, "Effective adsorptive removal of azo dyes over spherical ZnO nanoparticles," *J. Mater. Res. Technol.*, vol. 8, no. 1, pp. 713–725, Jan. 2019, doi: 10.1016/j.jmrt.2018.06.002.
- [9] A. I. Abd-Elhamid *et al.*, "Enhanced removal of cationic dye by eco-friendly activated biochar derived from rice straw," *Appl. Water Sci.*, vol. 10, no. 1, p. 45, Jan. 2020, doi: 10.1007/s13201-019-1128-0.
- [10] K. G. Akpomie and J. Conradie, "Biosorption and regeneration potentials of magnetite nanoparticle loaded *Solanum tuberosum* peel for celestine blue dye," *Int. J. Phytoremediation*, vol. 23, no. 4, pp. 347–361, Mar. 2021, doi: 10.1080/15226514.2020.1814198.
- [11] M. Pita, K. J. Fernández-Andrade, S. Quiroz-Fernández, J. M. Rodríguez-Díaz, and C. A. Díaz, "Assessment of biomass as an effective adsorbent for the removal of pharmaceutical compounds: A literature review," *Case Stud. Chem. Environ. Eng.*, vol. 9, p. 100596, Jun. 2024, doi: 10.1016/j.csee.2023.100596.
- [12] J. Bayuo, M. Rwiza, and K. Mtei, "A comprehensive review on the decontamination of lead(II) from water and wastewater by low-cost biosorbents," *RSC Adv.*, vol. 12, no. 18, pp. 11233–11254, 2022, doi: 10.1039/D2RA00796G.
- [13] Md. R. Khan, S. M. Hoque, K. F. B. Hossain, Md. A. B. Siddique, Md. K. Uddin, and Md. M. Rahman, "Green synthesis of silver nanoparticles using *Ipomoea aquatica* leaf extract and its cytotoxicity and antibacterial activity assay," *Green Chem. Lett. Rev.*, vol. 13, no. 4, pp. 303–315, Oct. 2020, doi: 10.1080/17518253.2020.1839573.
- [14] G. Das, J. K. Patra, N. Basavegowda, Chethala. N. Vishnuprasad, and H.-S. Shin, "Comparative study on antidiabetic, cytotoxicity, antioxidant and antibacterial properties of biosynthesized silver nanoparticles using outer peels of two varieties of *Ipomoea batatas* (L.) Lam," *Int. J. Nanomedicine*, vol. Volume 14, pp. 4741–4754, Jul. 2019, doi: 10.2147/IJN.S210517.
- [15] C. R. Silva-Correa *et al.*, "Potential Anticancer Activity of Bioactive Compounds from *Ipomoea batatas*," *Pharmacogn. J.*, vol. 14, no. 3, pp. 650–659, Jun. 2022, doi: 10.5530/pj.2022.14.84.
- [16] E. Rohaeti, "Application of Silver Nanoparticles Synthesized by Using *Ipomoea batatas* L. Waste to Improve Antibacterial Properties and Hydrophobicity of Polyester Cloths".
- [17] Y. R. Im, I. Kim, and J. Lee, "Phenolic Composition and Antioxidant Activity of Purple Sweet Potato (*Ipomoea batatas* (L.) Lam.): Varietal Comparisons and Physical Distribution," *Antioxidants*, vol. 10, no. 3, p. 462, Mar. 2021, doi: 10.3390/antiox10030462.
- [18] K. G. Akpomie and J. Conradie, "Biogenic and chemically synthesized *Solanum tuberosum* peel-silver nanoparticle hybrid for the ultrasonic aided adsorption of bromophenol blue dye," *Sci. Rep.*, vol. 10, no. 1, p. 17094, Oct. 2020, doi: 10.1038/s41598-020-74254-y.
- [19] S. Zhu, H. Sun, T. Mu, Q. Li, and A. Richel, "Preparation of cellulose nanocrystals from purple sweet potato peels by ultrasound-assisted maleic acid hydrolysis," *Food Chem.*, vol. 403, p. 134496, 2023, doi: https://doi.org/10.1016/j.foodchem.2022.134496.
- [20] K. Radosz-Soliwoda *et al.*, "The role of tannic acid and sodium citrate in the synthesis of silver nanoparticles," *J. Nanoparticle Res.*, vol. 19, no. 8, p. 273, Aug. 2017, doi: 10.1007/s11051-017-3973-9.
- [21] B. J. Wiley, S. H. Im, Z.-Y. Li, J. McLellan, A. Siekkinen, and Y. Xia, "Maneuvering the Surface Plasmon Resonance of Silver Nanostructures through Shape-Controlled Synthesis," *J. Phys. Chem. B*, vol. 110, no. 32, pp. 15666–15675, Aug. 2006, doi: 10.1021/jp0608628.
- [22] K. Okaiyeto, M. O. Ojemaye, H. Hoppe, L. V. Mabinya, and A. I. Okoh, "Phytofabrication of Silver/Silver Chloride Nanoparticles Using Aqueous Leaf Extract of *Oedera genitifolia*: Characterization and

Antibacterial Potential,” *Molecules*, vol. 24, no. 23, p. 4382, Nov. 2019, doi: 10.3390/molecules24234382.

- [23] Th. B. Devi and M. Ahmaruzzaman, “Bio-inspired sustainable and green synthesis of plasmonic Ag/AgCl nanoparticles for enhanced degradation of organic compound from aqueous phase,” *Environ. Sci. Pollut. Res.*, vol. 23, no. 17, pp. 17702–17714, Sep. 2016, doi: 10.1007/s11356-016-6945-1.
- [24] Y. Yang, T. Zhao, and T. Zhang, “Synthesis of silver nanoparticles via traditional Chinese medicine and evaluation of their antibacterial activities,” *RSC Adv.*, vol. 11, no. 47, pp. 29519–29526, 2021, doi: 10.1039/D1RA05562C.



Mirza Ardella Saputra was born in Grobogan, Central Java and she is a lecturer in Nanotechnology Engineering, Faculty of Advanced Technology and Multidiscipline, Universitas Airlangga. Her educational background includes Bachelor Degree and Master Degree in natural product organic chemistry from Chemistry Department of Universitas Airlangga and Universiti Teknologi Malaysia, respectively. Following that she studied the development of organic reactions for the synthesis of small molecules from Chemistry Department, Louisiana State University, USA and subsequently a postdoctoral training in the Chemistry and Biochemistry Department, San Diego State University, USA. Her current research involves nanocatalysis using various nanomaterials for organic pollutant removal via chemical reduction, photodegradation, and through adsorption processes.



Bastoni Semendawai was born in Jambi, Sumatra, and he is a former student of Nanotechnology Engineering, Faculty of Advanced Tehcnology and Multidiscipline, Universitas Airlangga, graduated in 2024. He is interested in the field of nanoengineering for environmental remediation and in petroleum industry. Email: semendawaibastoni@gmail.com.



Mochamad Lutfi Firmansyah was born in Bandung, Indonesia. He is a lecturer in Nanotechnology Engineering, Faculty of Advanced Technology and Multidiscipline, Universitas Airlangga. He graduated from Institut Teknologi Bandung in 2009 with chemistry degree and a master degree from Universiti Teknologi Malaysia. He then received his PhD from Kyushu University, Japan in 2019 from applied chemistry major. He is currently doing postdoc at King Fahd University of Petroleum and Minerals, UAE. His research interest revolves in solid adsorbent and ionic liquid and their application as adsorbent for heavy metal or any other pollutants. He is also working on metal recycling from electronic waste. Email: ml.firmansyah@ftmm.unair.ac.id.